Electronic Supplementary Information

Improved Pharmacokinetics of Mercaptopurine Afforded by a Thermally Robust Hemihydrate

Kortney M. Kersten,[a] Adam J. Matzger[a,b]

[a] Department of Chemistry, [b] Macromolecular Science and Engineering,
University of Michigan, 930 North University Avenue, Ann Arbor, Michigan 48109-1055,
United States

Table of Contents

SI 1. Experimental

Materials

Mercaptopurine monohydrate was obtained from Acros. Methanol was obtained from Fisher Scientific. Anhydrous methanol, 99.8%, AcroSeal, was obtained from Acros. All reagents were used without further purification.

Crystallization

Crystals of the monohydrate form were grown from methanol solutions (4 mg/mL) heated to 80 °C to dissolve all solids. Solutions were passed through a syringe filter (9 mL) into a 20 mL vial containing 5 mL H_2O. Vials were sealed and yellow block-shaped crystals grew after two days at room temperature.

Crystals of the hemihydrate form were grown from methanol solutions (4 mg/mL) heated to 80 °C to dissolve all solids. Solutions were passed through a syringe filter (4.5 mL) into a 20 mL vial containing 0.5 mL H_2O. Vials were sealed and yellow needle crystals grew after two days at room temperature.

Crystals of the anhydrate form were grown from anhydrous methanol solutions (4 mg/mL) in closed vials purged with N_2 heated to 80 °C to dissolve all solids. Solutions were passed through a syringe filter into new 30 mL vials. Solutions were concentrated under high vacuum to promote crystallization. Yellow needle crystals grew after several days at room temperature.

Computation of Vibrational Modes

Computation of the vibrational modes of isolated 6-mercaptopurine were performed in Spartan ‘14 V 1.1.2. The energy of the initial structure was minimized using molecular mechanics (MMFF). The equilibrium geometry was calculated using density functional theory B3LYP with the basis set 6-31G* in the gas phase and the predicted Raman spectra was calculated using the same methods.

Raman Spectroscopy

Raman spectra were collected using a Renishaw inVia Raman Microscope equipped with a Leica microscope, 633 nm laser, 1800 lines/mm grating, 50 μm slit, and a RenCam CCD detector. Spectra were collected in extended scan mode with a range of 300-1600 cm^{-1} and then analyzed using the WiRE 3.4 software package (Renishaw). Calibration was performed using a silicon standard.

Raman spectra during slurry conversion were collected using a Kaiser Optical Systems Raman Rxn Microprobe equipped with a Multi-Rxn non-contact optic, 785 nm laser, and a multi-channel CCD detector. Spectra were collected with a range of 150-3425 cm^{-1} and then analyzed

using the HoloGRAMS 4.1 software package (Kaiser). Calibration was performed using a HoloLab Calibration Accessory and a cyclohexane standard.

Powder X-Ray Diffraction (PXRD)

Powder X-Ray diffraction patterns were collected on a Bruker D8 Advance diffractometer using Cu-Kα radiation (λ = 1.54187 Å) and operating at 40 kV and 40 mA. Samples were prepared by grinding the crystals and pressing onto a glass slide. The pattern was collected by scanning 2θ from 5° to 60° with a step size of 0.02° and a step speed of 0.9 seconds. Powder patterns were processed using Jade 8 XRD Pattern Processing, Identification & Quantification analysis software (Materials Data, Inc).[1] All powder patterns were compared to their respective simulated powder patterns from single crystal X-ray diffraction structures and were found to be in substantial agreement with the predicted patterns.

Variable temperature PXRD data were collected on a Rigaku SmartLab diffractometer using Cu-Kα radiation (λ = 1.54187 Å) and operating at 40 kV and 44 mA. Samples were placed on a glass cover slip on top of a copper block that was heated at 2 °C/min using a J-KEM Model 210 temperature controller. The setup was covered with a housing of Kapton to keep heat in but allow X-rays to penetrate. The spectrum was collected by scanning 2θ from 20 to 29° with a step size of 0.01° and a step speed of 0.1 seconds. Powder patterns were processed using Jade 8 XRD Pattern Processing, Identification & Quantification analysis software.[1]

For comparison of the hemihydrate simulated powder pattern with the experimental, the low temperature unit cell constants were adjusted to the collected room temperature unit cell. Low temperature: a= 9.361 Å, b= 11.069 Å, c= 13.091 Å, β= 110.30°. Room temperature: a= 9.356 Å, b= 11.031 Å, c= 13.187 Å, β= 110.515°.

Single Crystal Structure Determination

Single crystal X-ray diffraction data for the hemihydrate form was collected using a Rigaku AFC10K Saturn 944+ CCD-based X-ray diffractometer equipped with a low temperature device and Micromax-007HF Cu-target micro-focus rotating anode (λ = 1.54187 A) operated at 1.2 kW power (40 kV, 30 mA). The X-ray intensities were measured at 85(1) K with the detector placed at a distance 42.00 mm from the crystal. The data was processed with CrystalClear 2.0 (Rigaku)[2] and corrected for absorption. The structure was solved and refined with the Bruker SHELXTL (version 2008/4)[3] software package, using the space group P2(1)/n with Z = 4 for the formula $2(C_2H_4N_4S), (H_2O)$. All non-hydrogen atoms were refined anisotropically with the hydrogen atoms placed in a combination of idealized and refined positions.

Differential Scanning Calorimetry (DSC)

Thermograms of the monohydrate and hemihydrate forms were recorded on a TA Instruments Q20 DSC. All experiments were run in Tzero™ hermetic aluminum DSC pans and studied under a nitrogen purge with a heating rate of 10 °C/min, while covering the temperature range of 35 °C

to 350 °C. Calibration of the instrument was performed using an indium standard. Thermograms were analyzed using TA Universal Analysis 2000, V 4.5A.

Thermograms of the monohydrate and hemihydrate forms using modulated heat flow were recorded on a TA instruments Q2000 DSC. All experiments were run in Tzero™ hermetic aluminum DSC pans and studied under a nitrogen purge with a heating rate of 5 °C/min, covering the temperature range of 35-250 °C. Oscillation was set at 1°C with a period of 60 seconds. Calibration of the instrument was performed using an indium standard. Thermograms were analyzed using TA Universal Analysis 2000, V 4.5A.

Karl Fisher Titration

The relative amounts of water, expressed as a percent (where 1 mg/g = 0.1 %), were determined via coulometric Karl Fisher titration using a Mettler Toledo C20 Coulometric KF Titrator. In order to avoid reaction of methanol with the mercaptan functionality, the Hydranal- Coulomat AK anolyte for ketones was used.

Elemental Analysis

Elemental analysis was performed by Midwest Microlab, Inc, Indianapolis, IN. Found: C, 37.18; H, 3.2. N, 34.66 Calc. for $C_5H_5N_4S_1O_{0.5}$: C, 37.16%; H, 3.3%,; N, 34.68%.

Solubility

Solubility measurements were taken using a CrystalBreeder system (Technobis). Known amounts of solid compound and water were added to 0.3 mL clear round bottom vials equipped with a stir bar. The vials were sealed with a Teflon coated rubber crimped caps to prevent evaporation of solvent. Vials were loaded into one of the independently heated aluminum reactor blocks and turbidity measurements were taken using an LED light source and detector to measure particles in solution. Samples were heated to 85 °C at a rate of 0.2 °C/min, held at 85 °C for 30 minutes, and then cooled to 0 °C at a rate of 0.2 °C/min. Clear points were calculated based on the temperature at which 100% transmittance of solution was reached. Van't Hoff plots of concentration vs. time were produced from the data using CrystalClear software (Technobis) to determine the solubility of each form at different temperatures.

Intrinsic Dissolution Rates

Intrinisic Dissolution Rates (IDR) were calculated using the μIDR™ miniature rotating disk method with the Pion Rainbow Dynamic Dissolution Monitor® system. Standard solutions of known concentrations were used to create calibration curves for each medium. All values collected during dissolution were compared to these calibration curves. For dissolution, pellets of the anhydrate and hemihydrate were formed within metal disks using the Pion μIDR press with ~10mg of material, held to 150 psi for 5 minutes. The disks were submerged in 10 mL of solution medium, stirred at 300 rpm, and UV-Vis probes with a path length of 2 mm were submerged above the disks. A time dependent concentration curve was observed *in situ* using the

AuPRO software (Version 5.1.1.0). The lambda maximum for the absorbance of mercaptopurine is located at 324 nm in both media. The intrinsic dissolution rate of each form is calculated by determining the slope of the initial linear region of the curve (2-30 mins) and then utilizing the slope (dc/dt) in the following equation:

$$IDR = V\,\frac{dc}{dt} * \frac{1}{A_{disk}}$$

where V= 10 mL and A_{disk} = 0.071 cm^2. With water as the medium, 5 and 6 trials were averaged for the hemihydrate and anhydrate, respectively. For the 0.5% methyl cellulose solution, 4 trials were averaged for each form.

Pharmacokinetic Studies in Rats

Pharmacokinetic studies in rats were performed at Avastus Preclinical Services, Cambridge, MA. All procedures were performed in accordance with the Guide for Care and Use of Laboratory Animals and were approved by the Avastus Institutional Animal Care and Use Committee. Male Sprague-Dawley rats weighing 200-300 g were dosed with mercaptopurine via oral gavage with a dosing volume of 5 mL/kg and a dose of 30 mg mercaptopurine form/kg or via IV administration at a dosing volume of 5 mL/kg and a dose of 15 mg mercaptopurine monohydrate/kg. Each group consisted of three rats, with one oral administration group for each form of mercaptopurine, and one IV administration group using the monohydrate form for reference. Blood samples were collected at time points of 15, 30, 60, 120, 240 minutes as well as 8 and 24 hours post dose. An additional time point at 5 minutes was taken for the IV administration group. Samples were centrifuged and the decanted plasma samples were stored at -80 °C until analysis.

PK Data Analysis

The plasma samples were analyzed via LC-MS/MS using an Agilent 6410 mass spectrometer coupled with an Agilent 1200 HPLC and a CTC PAL chilled autosampler, all controlled by MassHunter software (Agilent). All plasma samples were crashed with three volumes of methanol containing an analytical standard and centrifuged to remove precipitated protein before analysis. Samples were compared to a calibration curve prepared in rat blank plasma. Separation was performed on a C18 reverse phase HPLC column (Kinetex PFP, 2.6 µm, 2.1 x 50 mm) using an acetonitrile-water gradient system and peaks were analyzed by MS using ESI ionization in MRM mode. Peak area ratio to internal standard is used to interpolate plasma concentration for each sample from the calibration curve of peak area internal standard ratio to concentration. Pharmacokinetic parameters were fit using a custom WinNonlin analysis with PO dosing analysis. Area under the curve (AUC) for mercaptopurine was also calculated using the custom WinNonlin analysis. C_{max} (maximum plasma concentration) and T_{max} (time to reach maximum plasma concentration) were determined by averaging the respective parameter for each form, via the following equations:

$$C_{max} = \frac{C_{\max rat\ A} + C_{\max rat\ B} + C_{\max rat\ C}}{3} \quad (1)$$

$$T_{max} = \frac{T_{\max rat\ A} + T_{\max rat\ B} + T_{\max rat\ C}}{3} \quad (2)$$

The bioavailability (% F) was calculated from the following equation:

$$F = \frac{oral\ AUC\ (\frac{\mu g}{mL}.hr)}{iv\ AUC\ (\frac{\mu g}{mL}.hr)}\ x\ \frac{iv\ Dose\ (\frac{mg}{kg})}{oral\ Dose\ (\frac{mg}{kg})}\ x\ 100 \quad (3)$$

F_{rel} was calculated with respect to the monohydrate form.

SI 2. Raman Spectroscopy

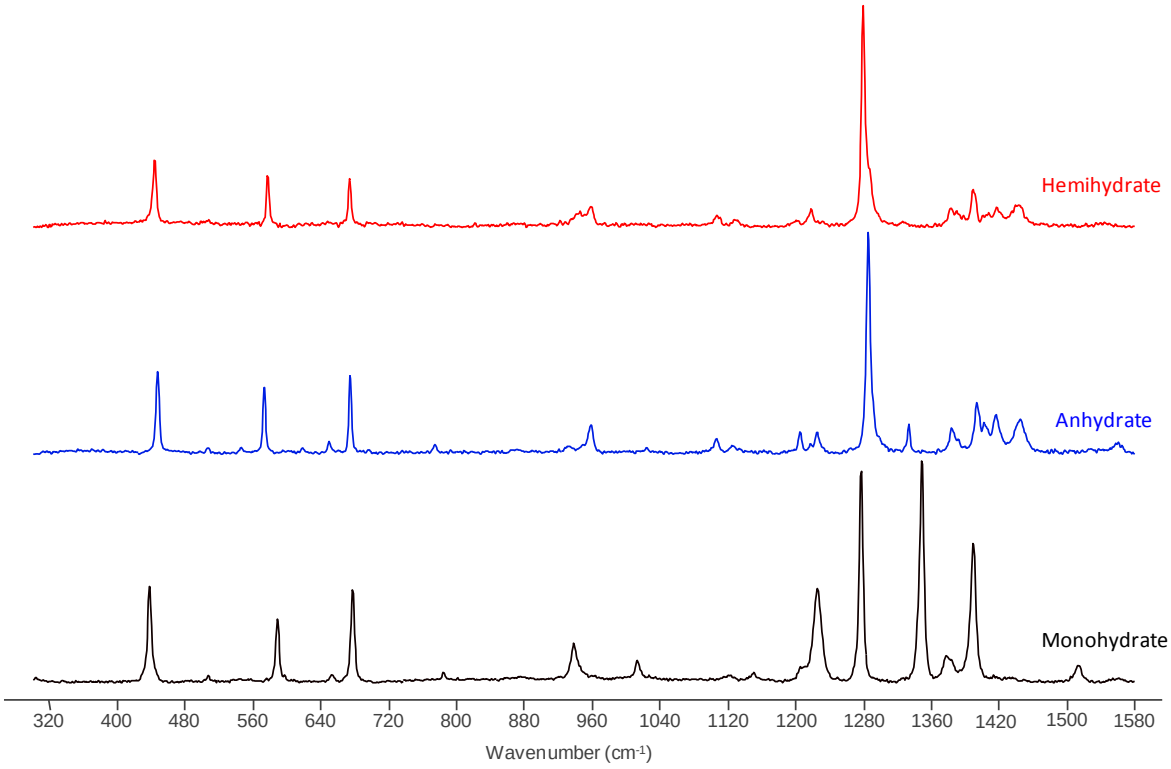

Figure S1. Raman spectra of the three forms of mercaptopurine.

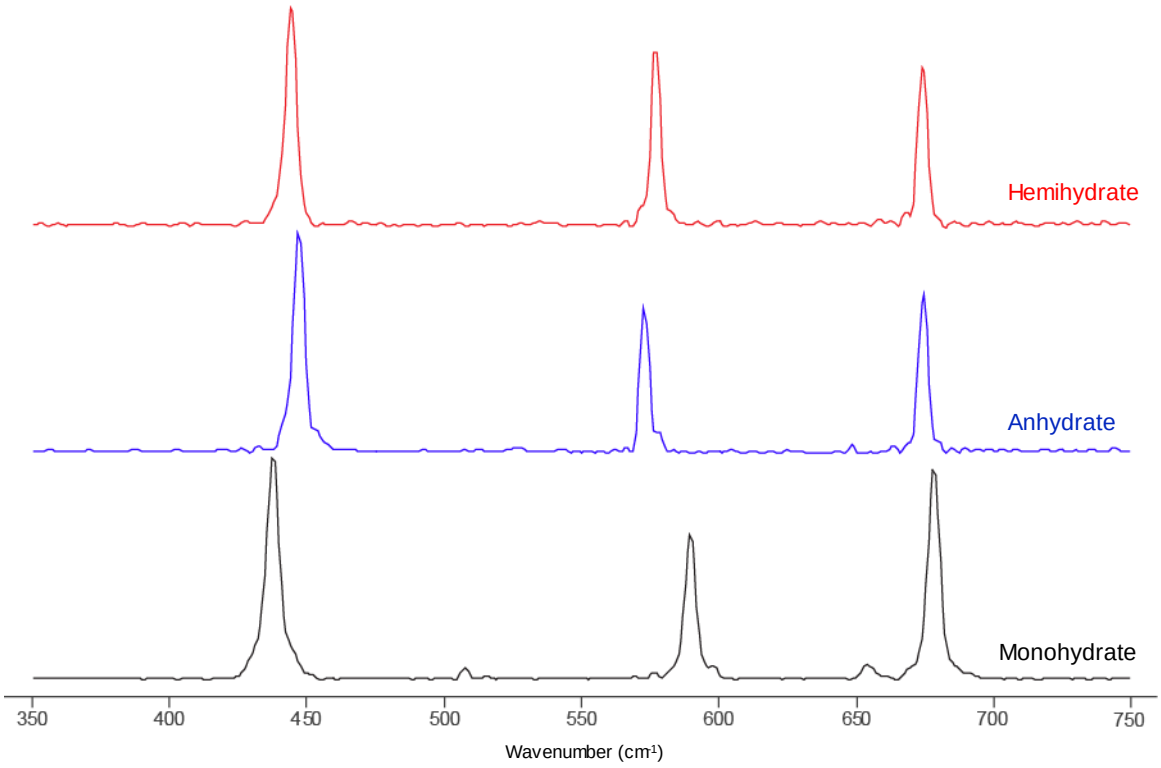

Figure S2. Raman spectra of the three forms of mercaptopurine showing the characteristic region of 350-750 cm^{-1}.

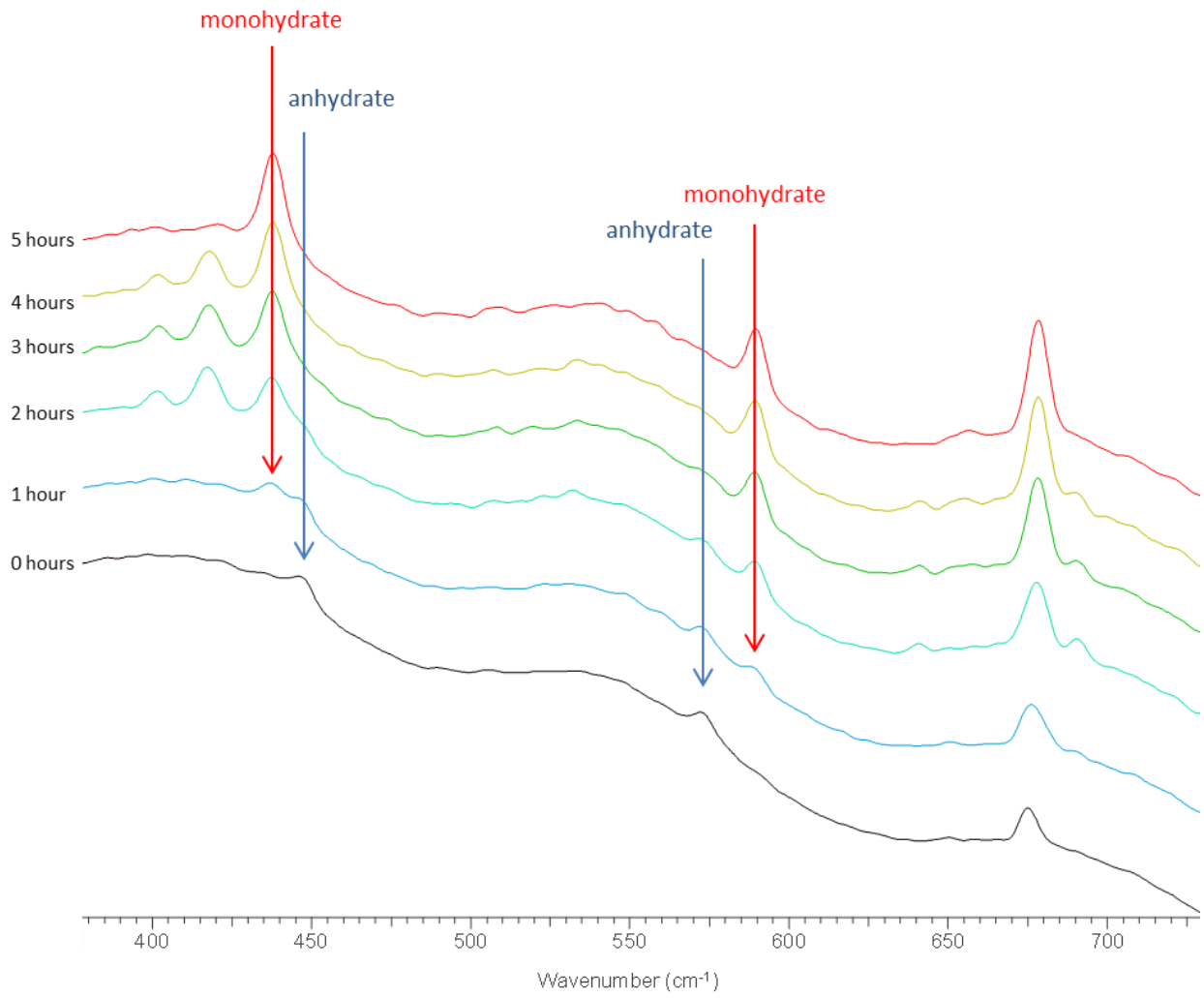

Figure S3. Raman spectra of slurry conversions for anhydrate converting to monohydrate.

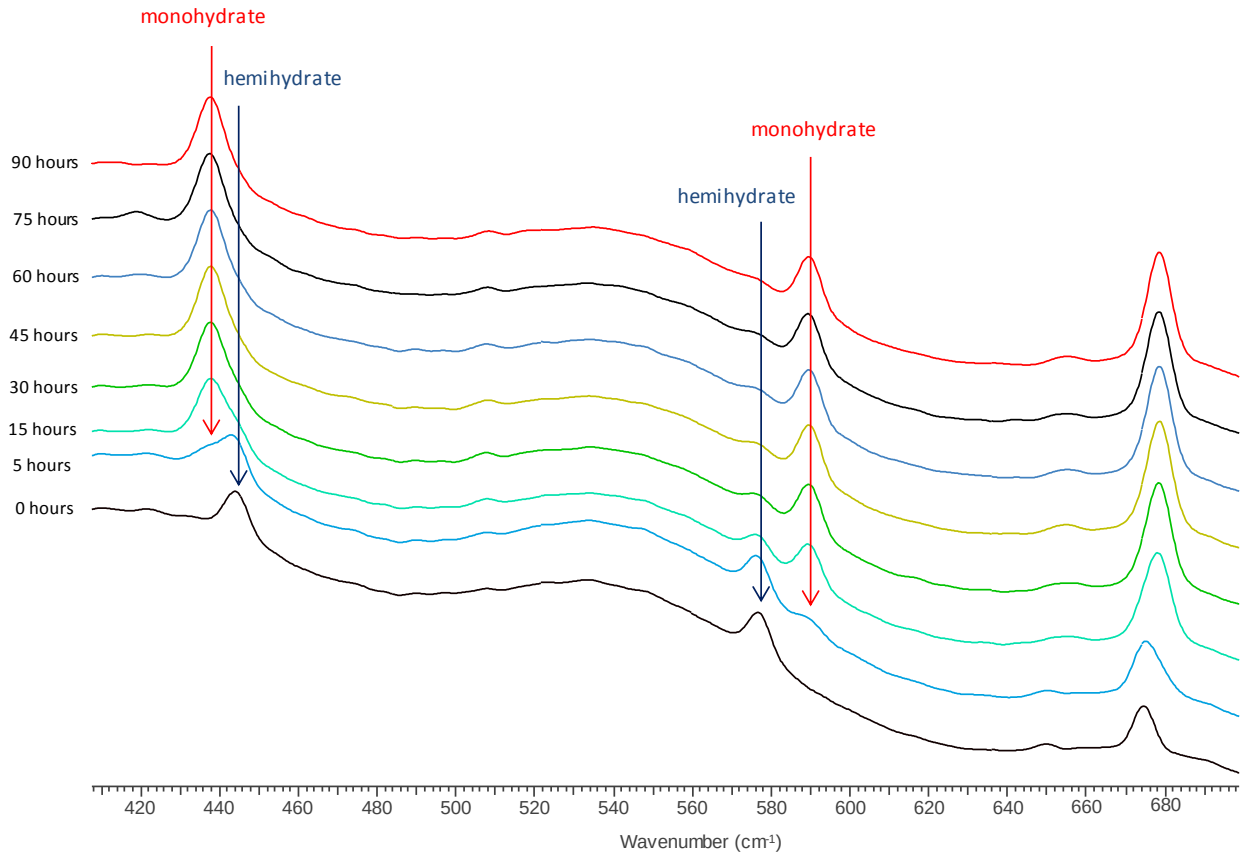

Figure S4. Raman spectra of slurry conversions for hemihydrate converting to monohydrate.

SI 3. Powder X-Ray Diffraction

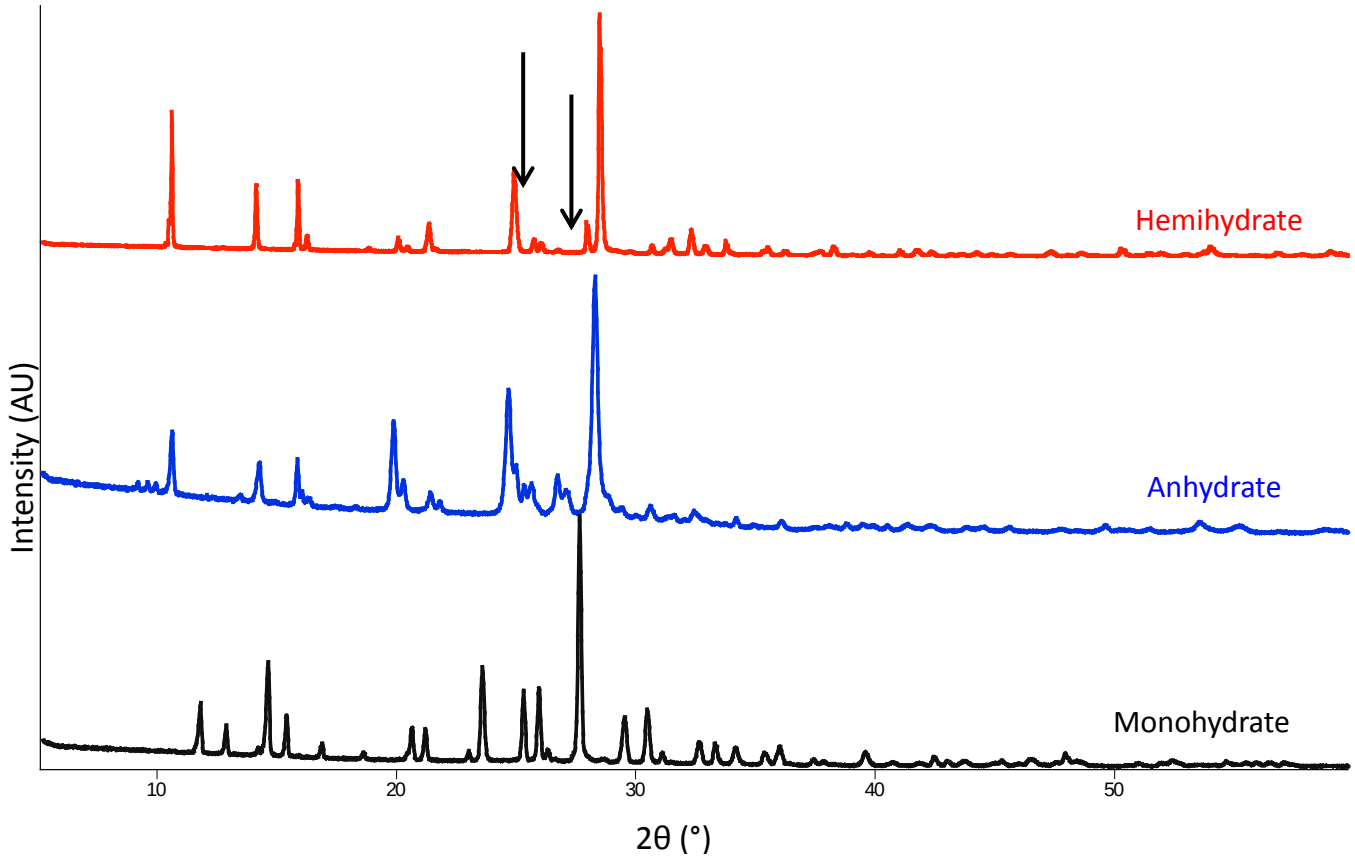

Figure S5. PXRD patterns of the three forms of mercaptopurine. Differences in the hemihydrate pattern from the anhydrate pattern are highlighted with arrows.

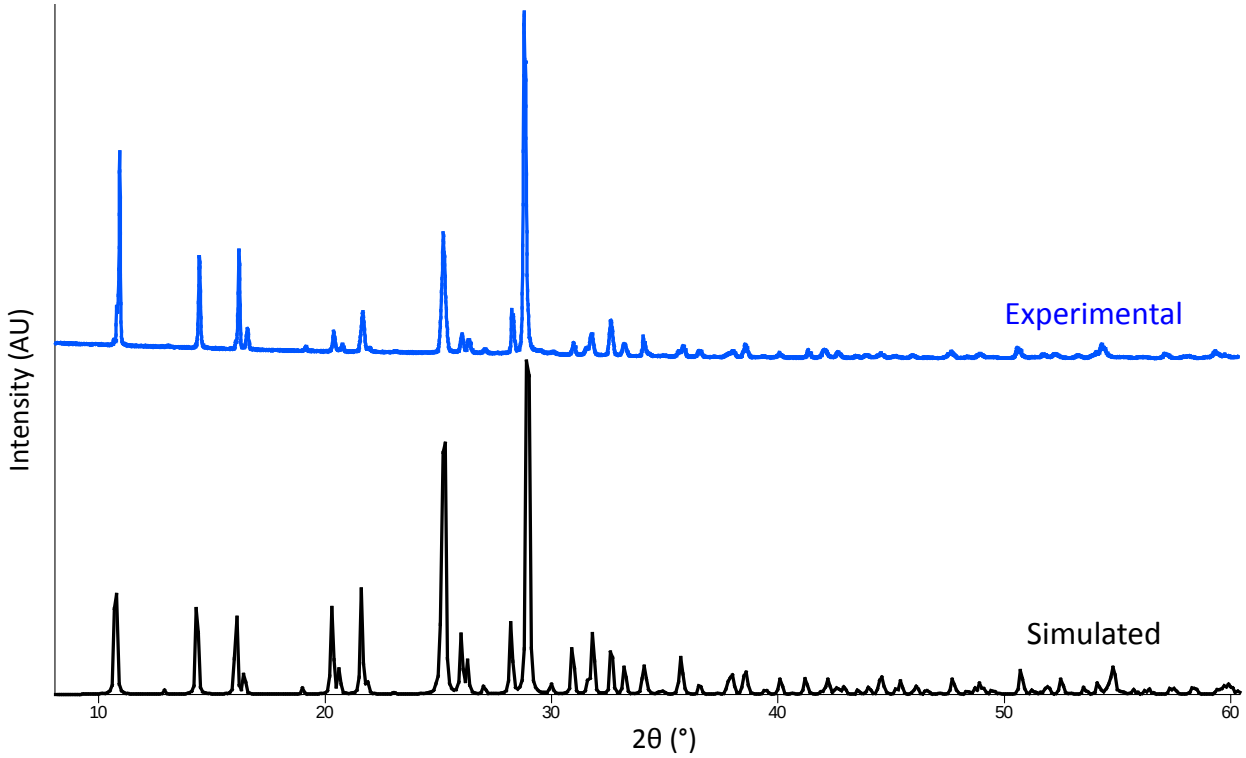

Figure S6. Simulated room temperature PXRD pattern and experimental PXRD pattern for the hemihydrate form.

SI 4. Single Crystal Data

Table S1. Crystallographic data for the three forms of mercaptopurine.

	Monohydrate	Anhydrate	Hemihydrate
Refcode or CCDC #	MERPUM[4]	RAKSIG[5]	1447142
Chemical formula	$C_5H_6N_4S_1O_1$	$C_5H_4N_4S_1$	$C_{10}H_{10}N_8S_2O_1$
Formula Weight (g/mol)	170.19	152.18	161.19
Crystal system	monoclinic	monoclinic	monoclinic
Space group	C2/c	$P2_1/n$	$P2_1/n$
a (Å) =	15.294 (2)	4.710 (1)	9.361 (13)
b (Å) =	7.731 (1)	11.123 (1)	11.069 (2)
c (Å) =	12.379 (1)	12.230 (1)	13.091 (9)
α (°) =	90	90	90
β (°) =	101	91.02	110.30
γ (°) =	90	90	90
V ($Å^3$) =	716.876	640.630	1272.71
Z' =	1.0	1.0	1.0
Z =	8.0	4.0	4.0
Temperature (K) =	283-303	183	85
Reflections Measured	-	-	2311
R factor (%)	-	-	4.2 (all)

Note: Monohydrate and anhydrate form data taken from the Crystallographic Structure Database (v. 5.36).

SI 5. Crystal Structure Comparison

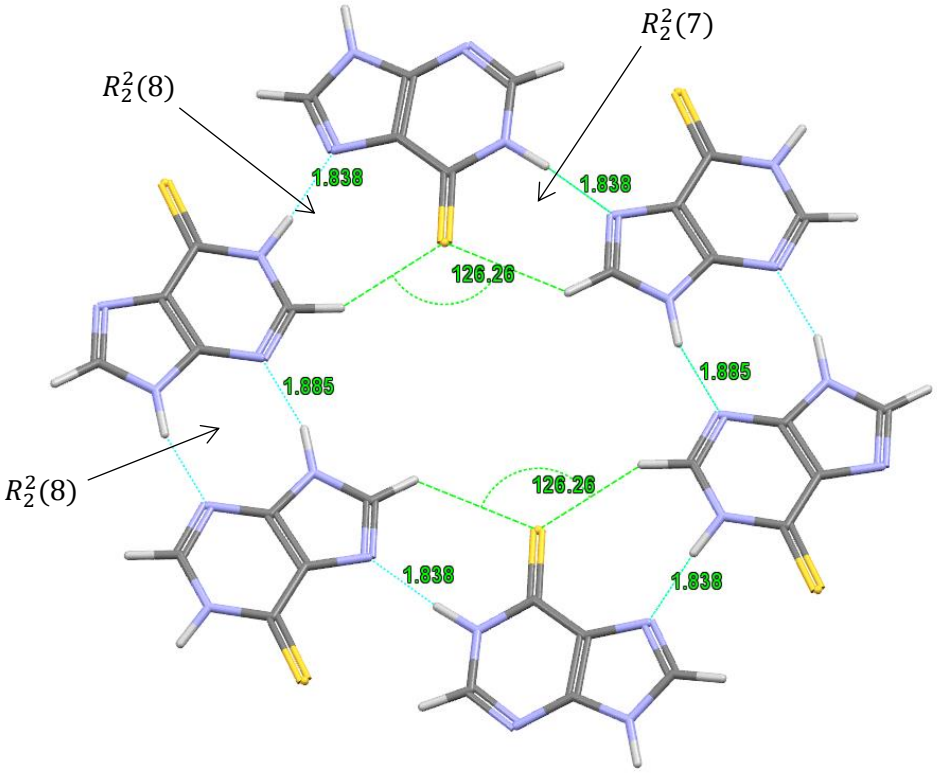

Figure S7. Selected area of mercaptopurine anhydrate structure with graph sets as well as select hydrogen bond distances and structural angles highlighted.

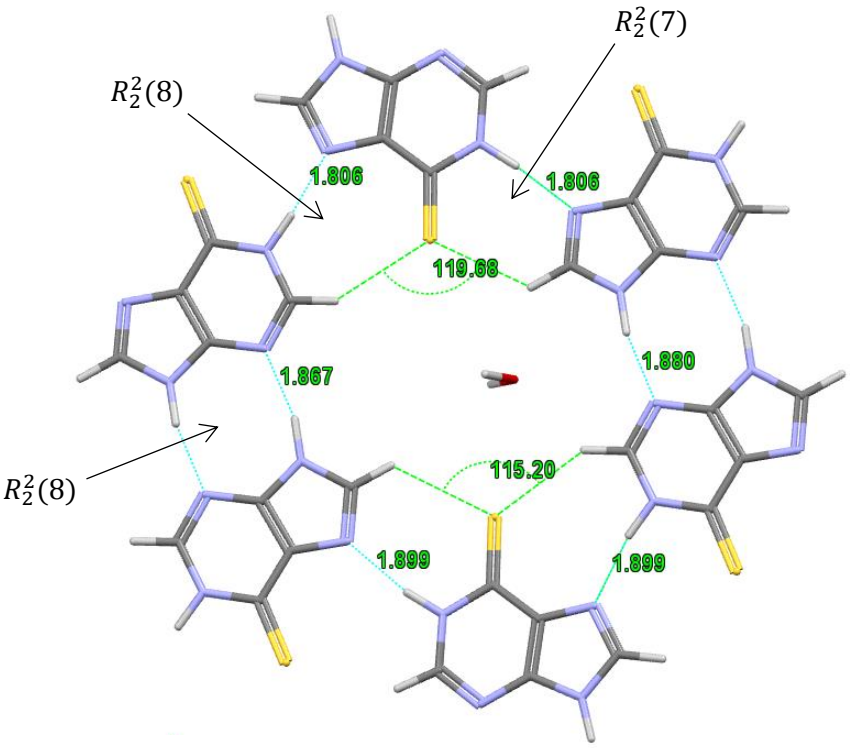

Figure S7. Selected area of mercaptopurine hemihydrate structure with graph sets as well as select hydrogen bond distances and structural angles highlighted.

SI 6. Differential Scanning Calorimetry

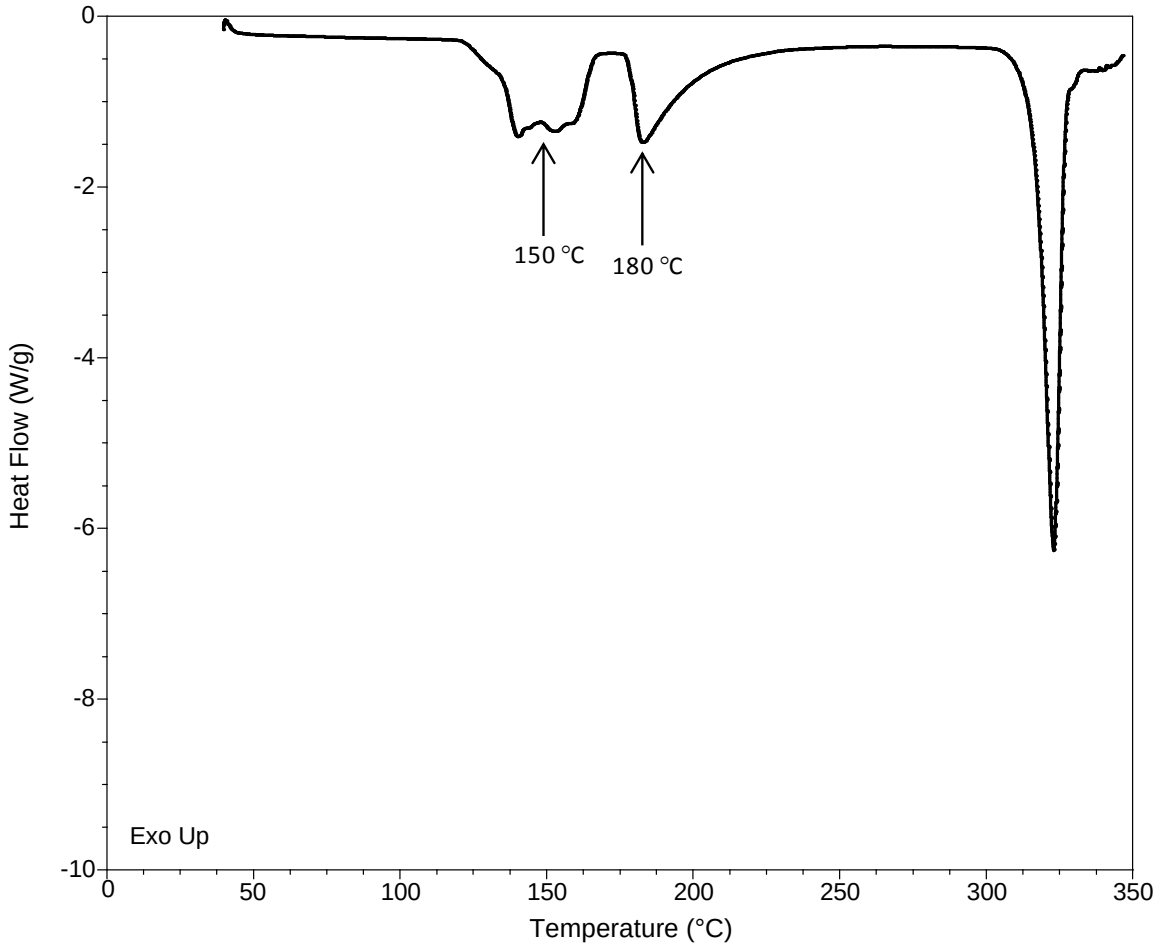

Figure S9. Differential scanning calorimetry thermogram for the monohydrate form of mercaptopurine in a sealed pan.

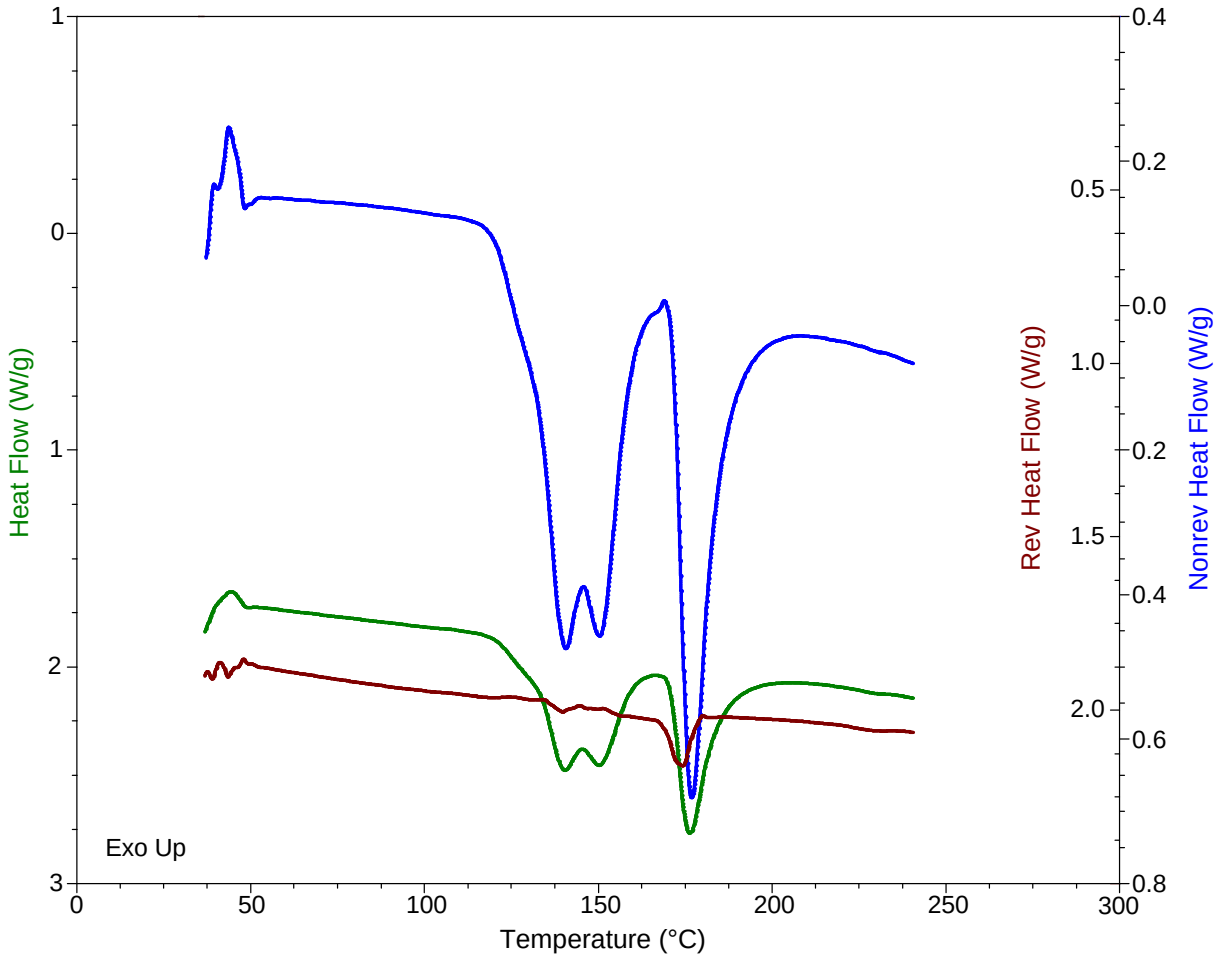

Figure S10. Modulated differential scanning calorimetry thermogram for the monohydrate form of mercaptopurine in a sealed pan.

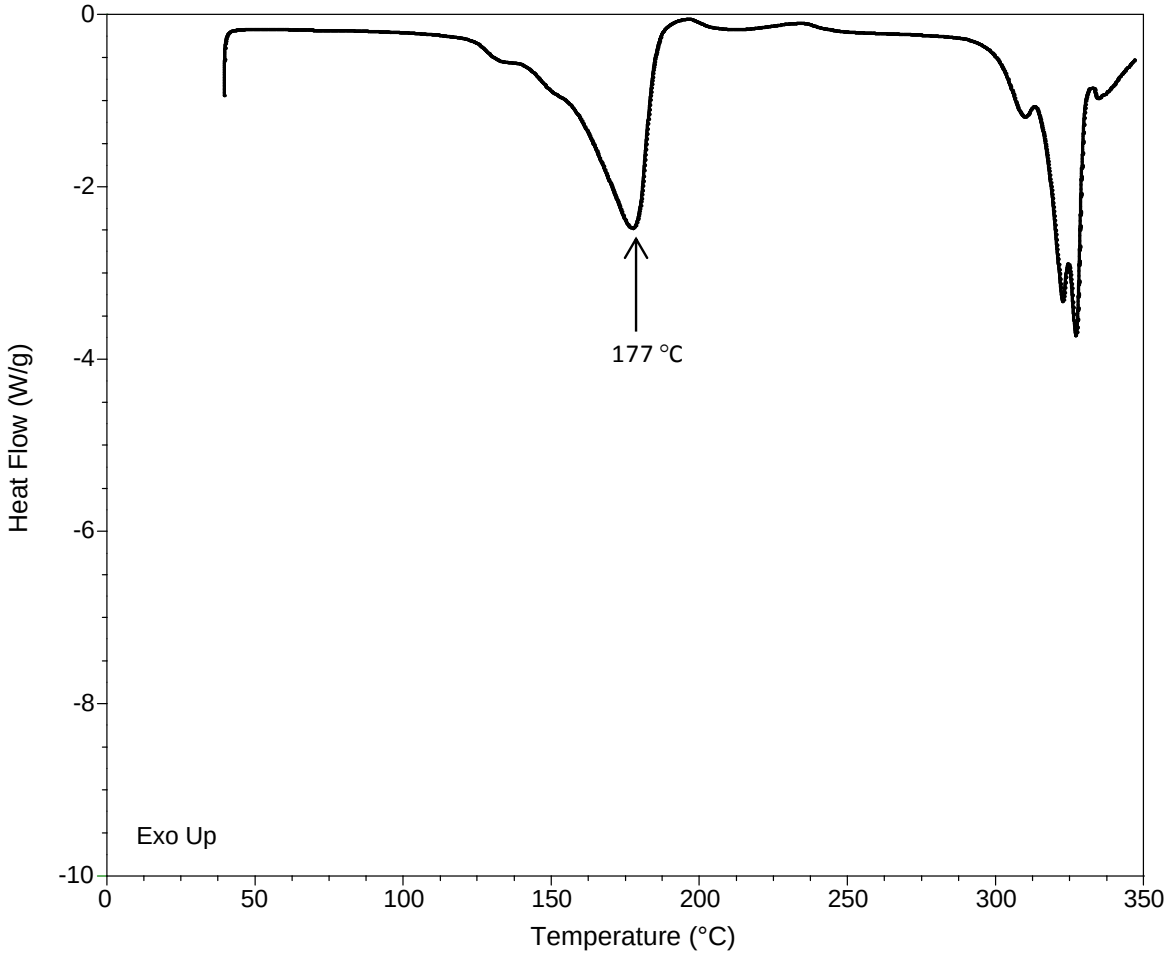

Figure S11. Differential scanning calorimetry thermogram the monohydrate form of mercaptopurine in a sealed pan with a hole poked in the lid.

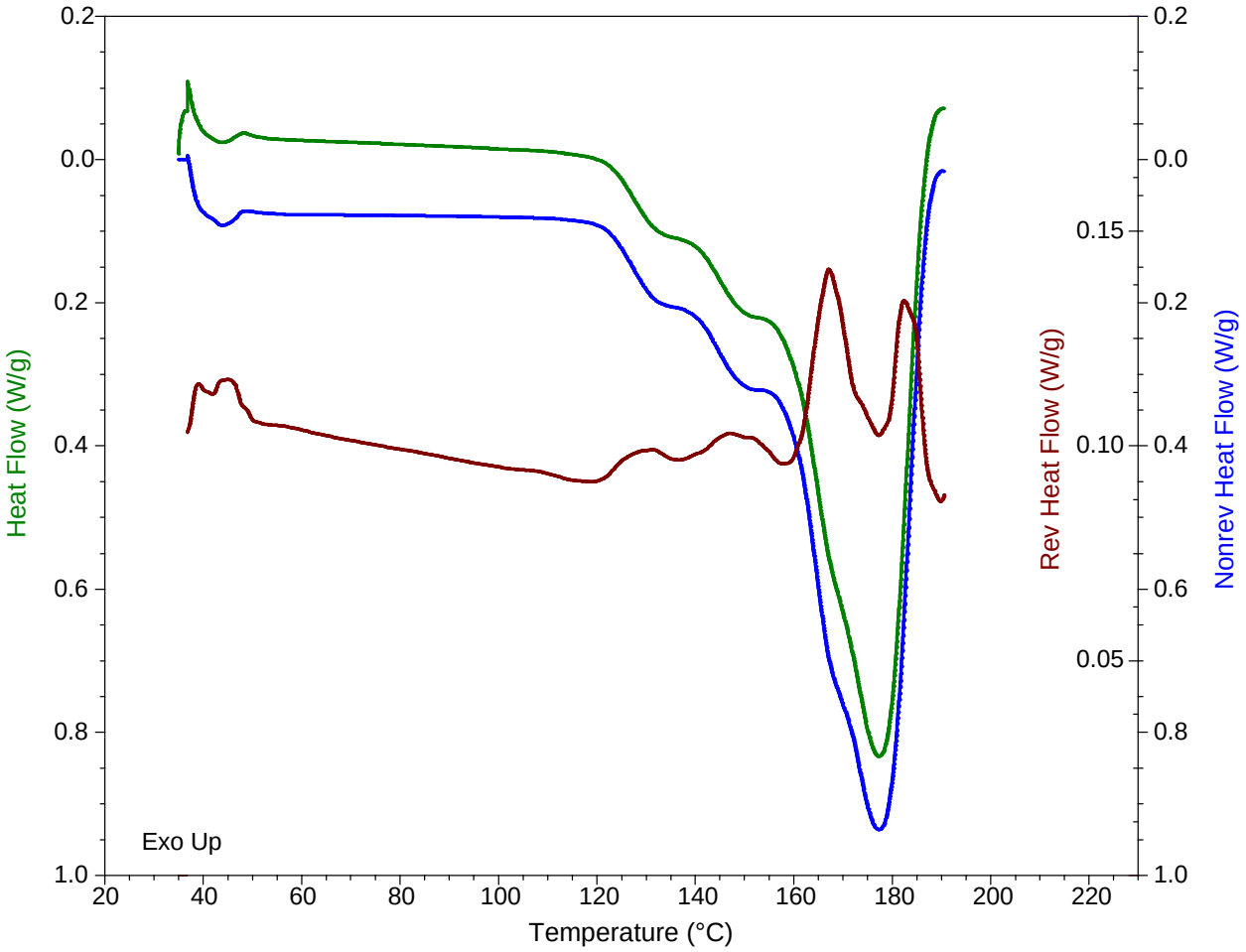

Figure S12. Modulated differential scanning calorimetry thermogram the monohydrate form of mercaptopurine in a sealed pan with a hole poked in the lid.

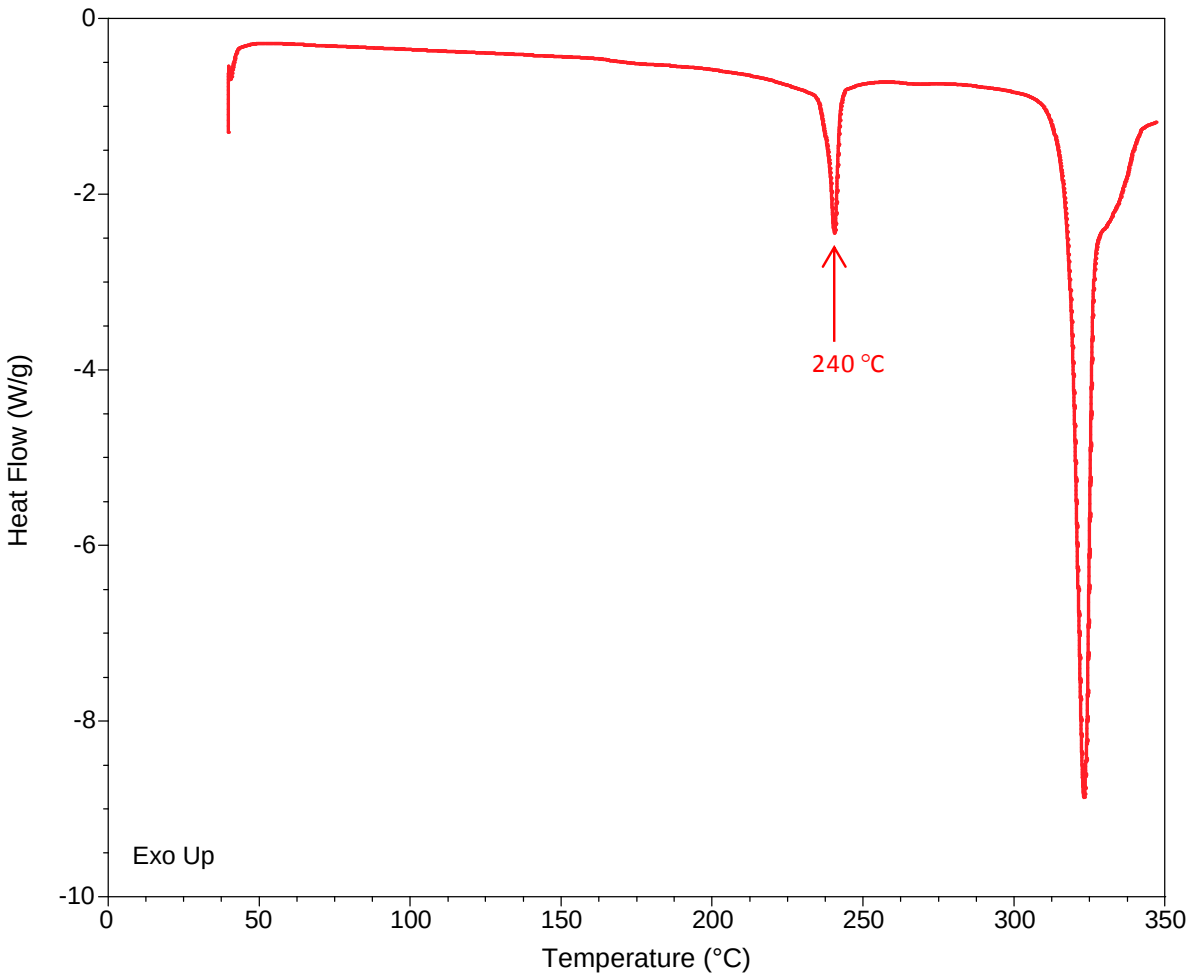

Figure S13. Differential scanning calorimetry thermogram for the hemihydrate form of mercaptopurine.

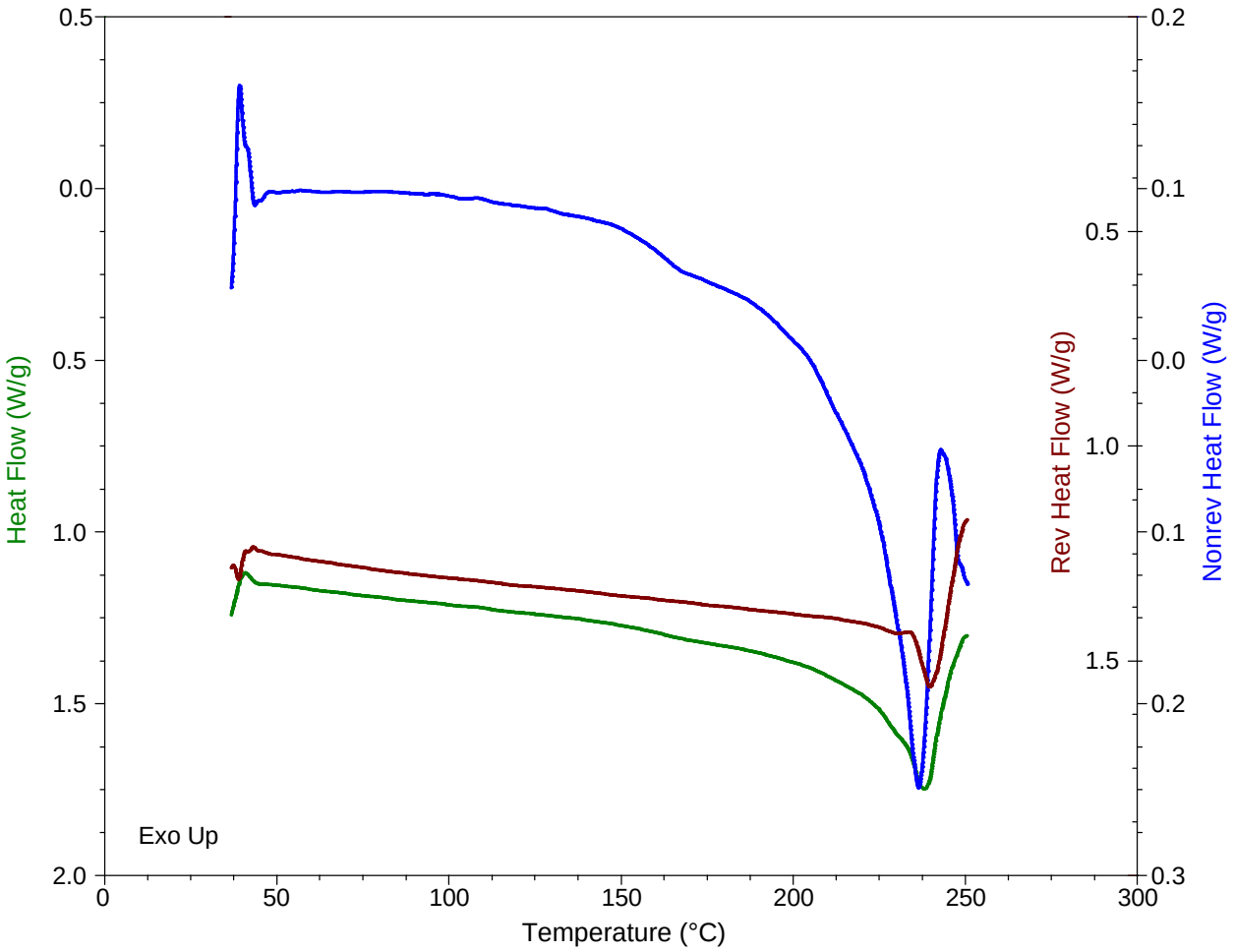

Figure S14. Modulated differential scanning calorimetry thermogram for the hemihydrate form of mercaptopurine.

SI 7. Thermogravimetric Analysis

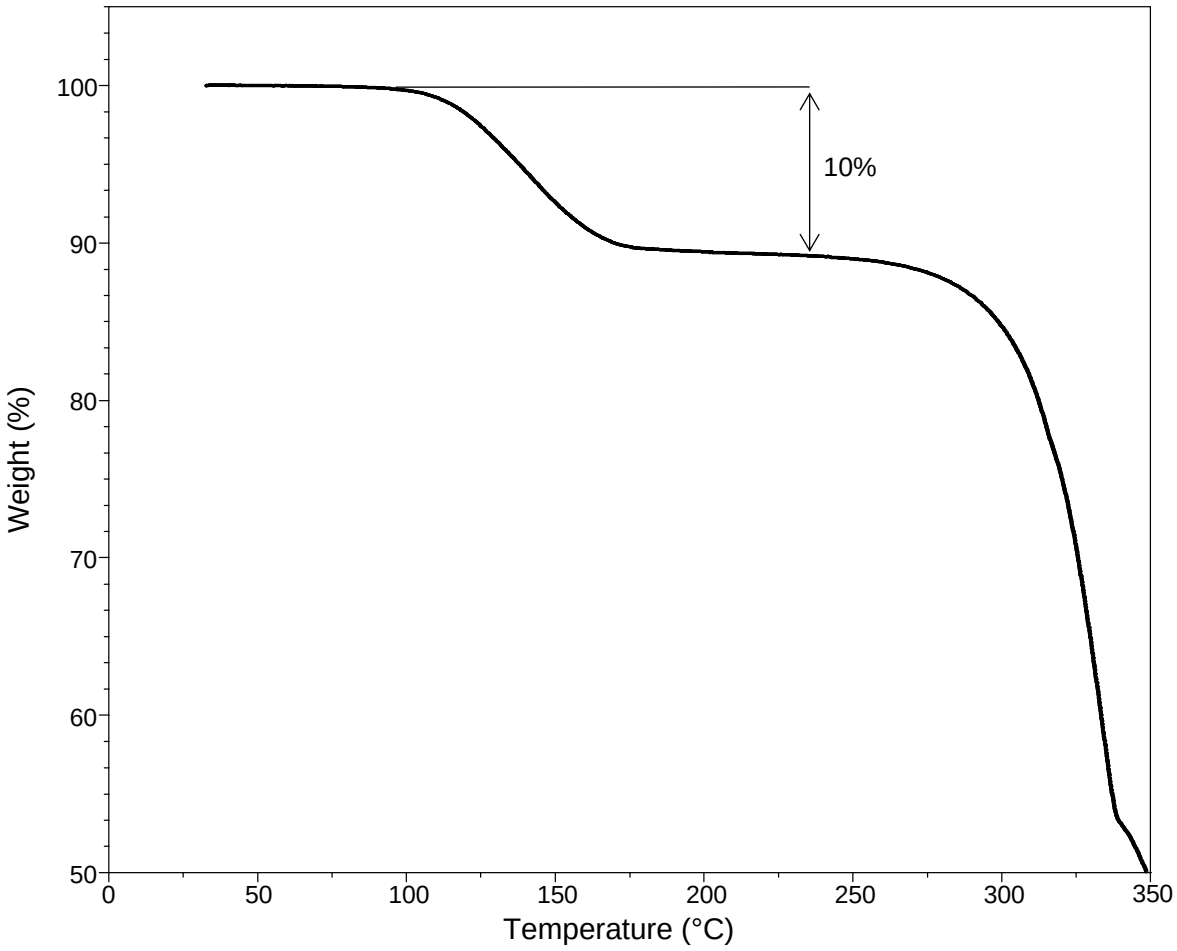

Figure S15. Thermogravimetric analysis of mercaptopurine monohydrate. Water loss of 10% occurs between 100-150 °C.

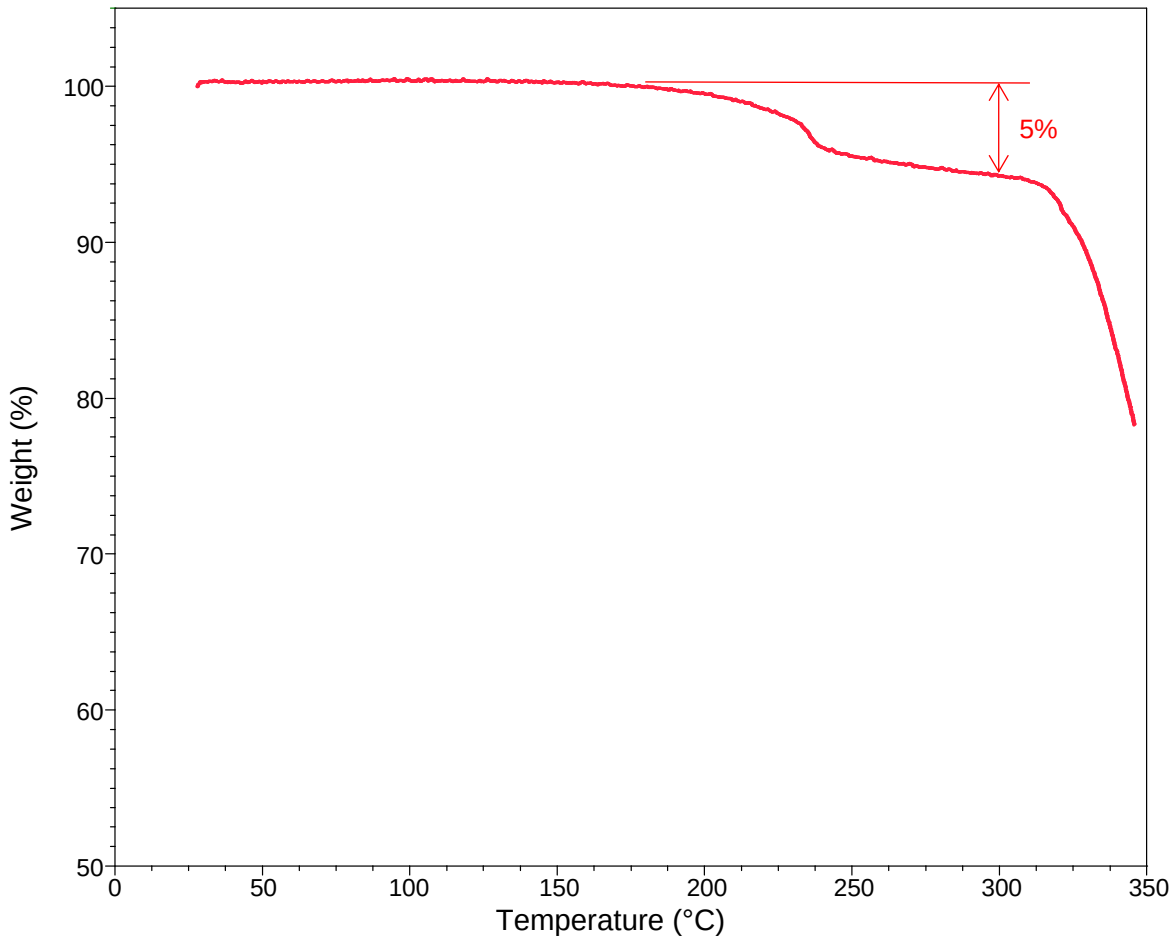

Figure S16. Thermogravimetric analysis of mercaptopurine hemihydrate. Water loss of 5% occurs between 200-250 °C.

SI 8. Intrinsic Dissolution Rate profile

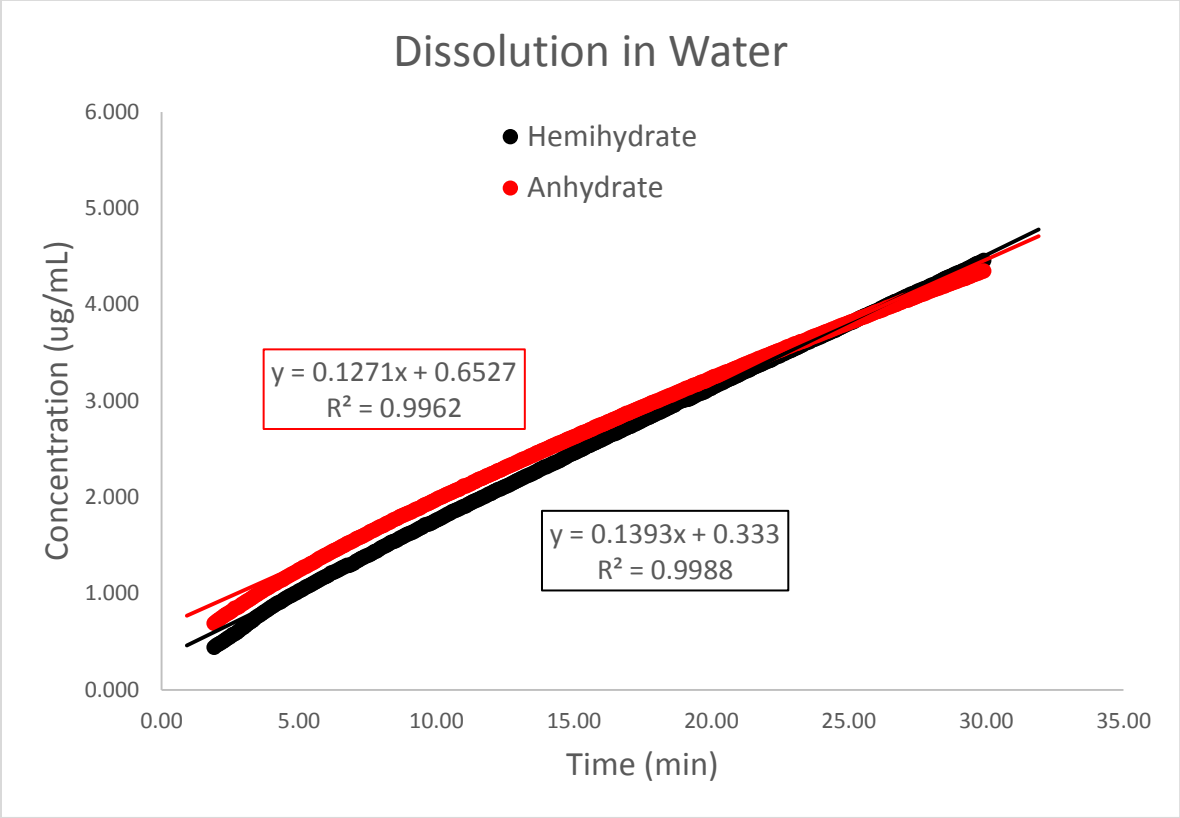

Figure S17. Average Intrinsic Dissolution Rate profile for the anhydrate and hemihydrate forms of mercaptopurine measured in water.

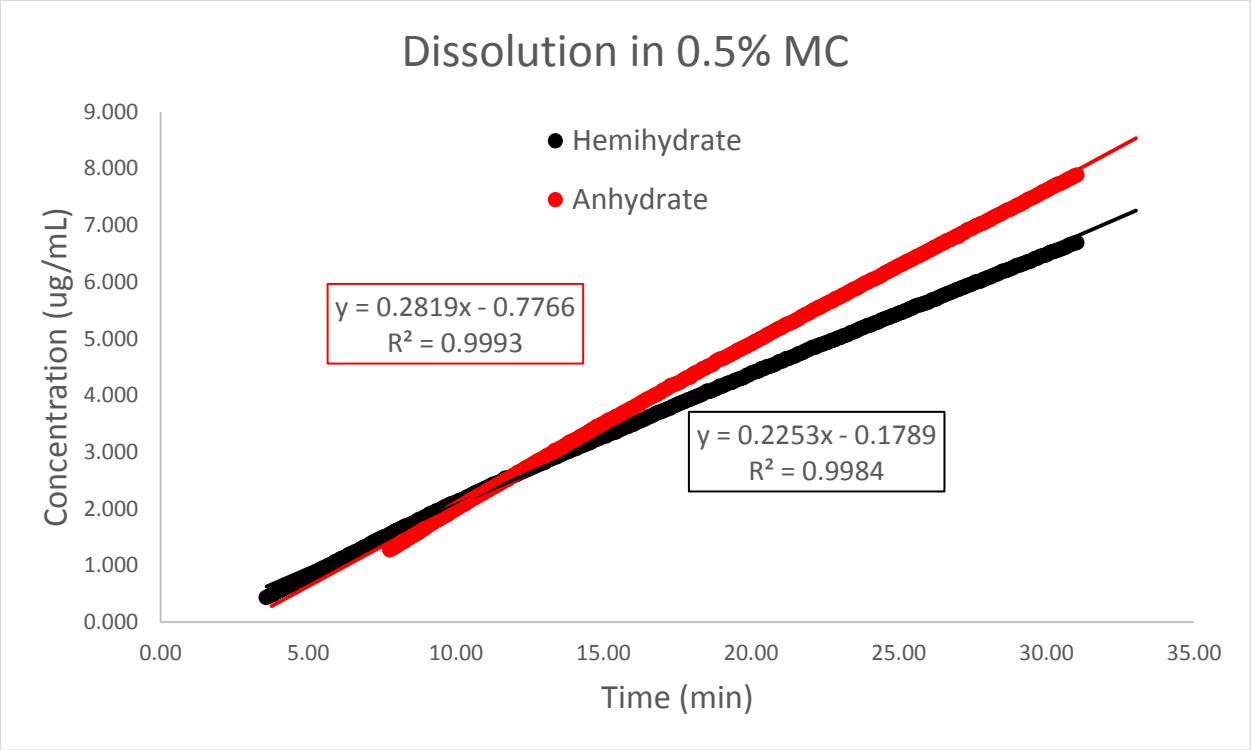

Figure S18. Average Intrinsic Dissolution Rate profile for the anhydrate and hemihydrate forms of mercaptopurine measured in 0.5% methyl cellulose solution.

SI 9. Additional Characterization Methods

Table S2. Karl Fisher analysis for the three forms of mercaptopurine.

Form	Theoretical % Water	Experimental % Water
Monohydrate	10.6	11.2
Hemihydrate	5.6	5.2
Anhydrate	0	0.7

Table S3. Elemental analysis for the hemihydrate form of mercaptopurine.

Element	Theoretical %	Experimental %
C	37.2	37.2
N	34.7	34.7
H	3.3	3.2

SI 10. References

(1) Jade Plus 8.2 ed.; Materials Data, Inc. 1995-2007.

(2) Crystal Clear Expert 2.0 r12, Rigaku Americas and Rigaku Corporation (2011), Rigaku Americas, 9009, TX, USA 77381-5209, Rigaku Tokyo, 196-8666, Japan.

(3) Sheldrick, G.M. SHELXTL, v. 2008/4; Bruker Analytical X-ray, Madison, WI, 2008.

(4) E. Sletten, J. Sletten, and L.H. Jensen. *Acta Crystallogr., Sect. B: Struct. Sci.*, 1969, **25,** 1330. "The Cambridge Structural Database: a quarter of a million crystal structures and rising".

(5) E. Gyr, H.W. Schmalle, and E. Dubler. CCDC 249870: Experimental Crystal Structure Determination, 2004, DOI: 10.5517/cc8d0bz. "The Cambridge Structural Database: a quarter of a million crystal structures and rising".